**ISCI, Volume *19***

## Supplemental Information

# Structural Basis of Mitochondrial Scaffolds by Prohibitin Complexes: Insight into a Role of the Coiled-Coil Region

**Takahiro Yoshinaka, Hidetaka Kosako, Takuma Yoshizumi, Ryo Furukawa, Yu Hirano, Osamu Kuge, Taro Tamada, and Takumi Koshiba**

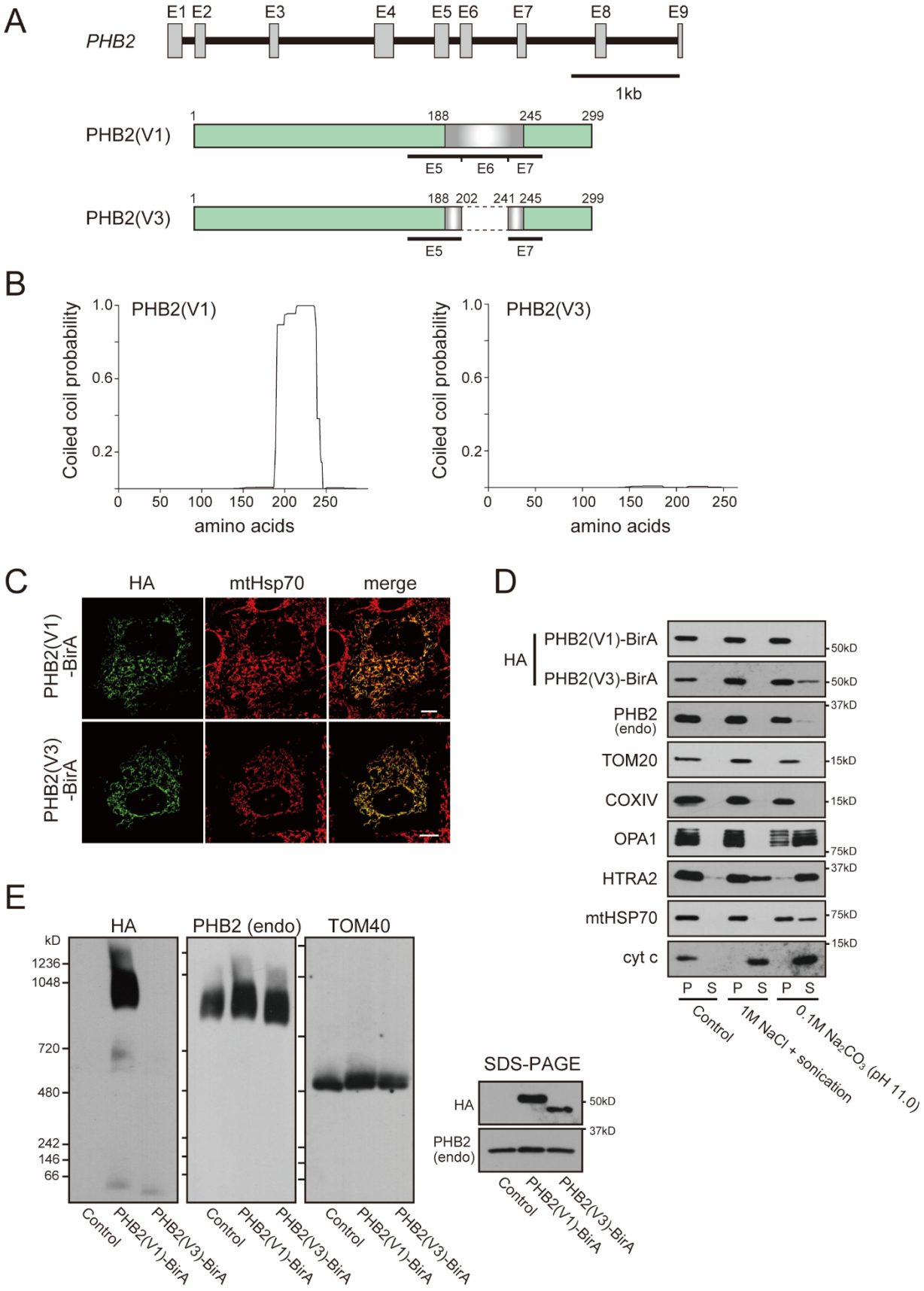
A
PHB2
E1 E2 E3 E4 E5 E6 E7 E8 E9
1kb
PHB2(V1)
1 188 245 299
E5 E6 E7
PHB2(V3)
1 188 202 241 245 299
E5 E7
B
PHB2(V1)
PHB2(V3)
Coiled coil probability
1.0
0.6
0.2
0 50 100 150 200 250
amino acids
C
HA
mtHsp70
merge
PHB2(V1) -BirA
PHB2(V3) -BirA
D
HA
PHB2(V1)-BirA
PHB2(V3)-BirA
PHB2 (endo)
TOM20
COXIV
OPA1
HTRA2
mtHSP70
cyt c
50kD
37kD
15kD
75kD
P S P S P S
Control
1M NaCl + sonication
0.1M Na2CO3 (pH 11.0)
E
HA
PHB2 (endo)
TOM40
kD
1236
1048
720
480
242
146
66
Control
PHB2(V1)-BirA
PHB2(V3)-BirA
SDS-PAGE
HA
PHB2 (endo)
50kD
37kD

**Figure S1, related to Figure 1. Schematic of PHB2 splice variants in humans**

(A) Schematic representation of the exon-intron structure of the human *PHB2* genome (top), and their translated two alternative splicing variants, V1 and V3, are shown. The V1 variant encodes a canonical sequence expressed with its complete polypeptide (middle), whereas the V3 variant lacks exon 6, abolishing the putative HR region (highlighted by gray) of the translated protein (bottom). The amino acid positions are indicated above the structure, and the dashed lines indicate the missing amino acids.

(B) Prediction results of the coiled-coil probability of PHB2 variants using the program COILS (Lupas et al., 1991). The V3 variant is predicted to not form the coiled-coil folding (right).

(C) Subcellular localization of BirA-fused constructs of PHB2 variants. The PHB2(V1)-BirA or PHB2(V3)-BirA constructs (HA-epitope-tagged at their C-terminus) were expressed in MEFs, and immunofluorescence against the HA epitope (left) was used to identify the V1- or V3-expressing cells and to determine their subcellular localizations (right). Mitochondria in the same cells were identified by staining with a monoclonal antibody against mtHsp70 (middle). Scale bar, 10 μm.

(D) Isolated mitochondria from HEK293 cells stably expressing either HA-tagged PHB2(V1)-BirA or PHB2(V3)-BirA were treated with either 1 M NaCl (plus sonication) or 0.1 M $Na_2CO_3$ (pH 11.0) for 30 min on ice. After centrifugation, the supernatant (S) and pellets (P) were analyzed by immunoblotting with antibodies against HA or against several mitochondrial proteins as indicated.

(E) Mitochondria isolated from HEK293 cells stably expressing either HA-tagged PHB2(V1)-BirA or PHB2(V3)-BirA were solubilized in BN-PAGE lysis buffer containing 0.5% (w/v) digitonin and analyzed by BN-PAGE and immunoblotted using the HA-, PHB2-, and TOM40-specific antibodies (left 3 panels). The abundance of BirA-fused proteins in each sample was confirmed by SDS-PAGE in parallel (right panels).

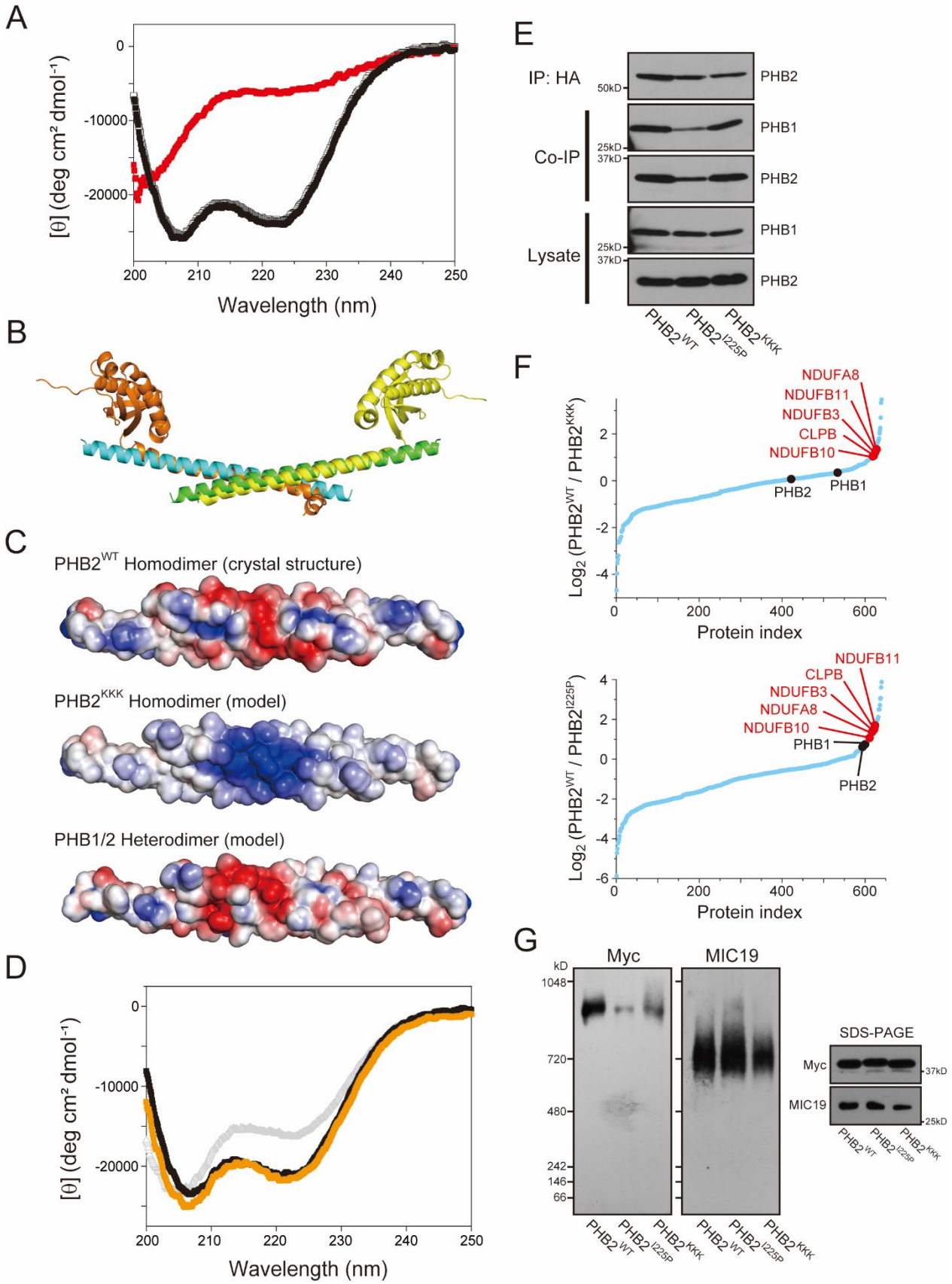
A
[θ] (deg cm² dmol⁻¹)
0
-10000
-20000
200
210
220
230
240
250
Wavelength (nm)
B
C
PHB2WT Homodimer (crystal structure)
PHB2KKK Homodimer (model)
PHB1/2 Heterodimer (model)
D
[θ] (deg cm² dmol⁻¹)
0
-10000
-20000
200
210
220
230
240
250
Wavelength (nm)
E
IP: HA
50kD
PHB2
Co-IP
25kD
37kD
PHB1
PHB2
Lysate
25kD
37kD
PHB1
PHB2
PHB2WT
PHB2I225P
PHB2KKK
F
Log2 (PHB2WT / PHB2KKK)
NDUFA8
NDUFB11
NDUFB3
CLPB
NDUFB10
PHB2
PHB1
2
0
-2
-4
0
200
400
600
Protein index
Log2 (PHB2WT / PHB2I225P)
NDUFB11
CLPB
NDUFB3
NDUFA8
NDUFB10
PHB1
PHB2
4
2
0
-2
-4
-6
0
200
400
600
Protein index
G
Myc
MIC19
kD
1048
720
480
242
146
66
PHB2WT
PHB2I225P
PHB2KKK
PHB2WT
PHB2I225P
PHB2KKK
SDS-PAGE
Myc
MIC19
37kD
25kD
PHB2WT
PHB2I225p
PHB2KKK

**Figure S2, related to Figure 2. Characteristics of the HR region of PHB2**

(A) CD spectra of $PHB2^{188-247}$. The sample at 4º C (filled square) was elevated temperature (1º C /min) at 60º C (red square), and then cooled down to 4º C (open square). CD spectra of $PHB2^{188-247}$ in far-UV region (200-250 nm) were measured at these different temperatures at pH 7.2.

(B) Superposition of the PHB2 coiled-coil and the coiled-coil region of p-stomatin PH1511p (PDB ID: 3BK6). Both structures are folded into a crystallographic two-fold symmetry, and the p-stomatin PH1511p anti-parallel dimers are shown in orange and yellow.

(C) An electrostatic potential map of the HR coiled-coil of PHB2 shows a highly charged surface (top). We designed a mutant ($PHB2^{KKK}$) in which three glutamic acid residues ($E^{229}$, $E^{231}$, and $E^{233}$) were substituted with lysine residues to remove the negatively-charged patch from the center of the structure (middle: model structure). Predicted PHB1-PHB2 heterodimer, which also forms a negative cluster, is shown (bottom: model structure). Basic regions are shown in blue, and acidic regions are shown in red.

(D) CD spectra of WT $PHB2^{188-247}$ (filled square) and its KKK variant (orange square) at 4º C in 1× PBS (pH 7.2). The CD spectrum of I225P variant was overlaid (gray triangle).

(E) Interaction of PHB2 variants with endogenous PHB1 or PHB2. Lysates of HEK293 cells stably expressing HA-tagged PHB2-BirA (WT) and its variants (I225P and KKK) were subjected to immunoprecipitation (IP) with HA monoclonal antibody followed by the analysis of immunoblots (Co-IP) with antibodies against PHB1 or PHB2.

(F) PHB2 coiled-coil is required to form the PHBs interactome assembly. A total of 640 proteins identified from BioID2 experiments (see Table S4) were plotted according to the abundance ratios ($log_2$) of $PHB2^{WT}/PHB2^{KKK}$ (top) or $PHB2^{WT}/PHB2^{I225P}$ (bottom) against individual proteins (Protein index) sorted by their ratios in ascending order.

(G) PHB2 coiled-coil is required to form the PHBs interactome assembly. Mitochondria isolated from HEK293 cells stably expressing Myc-tagged PHB2 (WT) and its variants (I225P and KKK) were solubilized in BN-PAGE lysis buffer containing 0.5% (w/v) digitonin, and analyzed by BN-PAGE and immunoblotted using the Myc- and MIC19-specific antibodies (left 2 panels). The abundance of the Myc-tagged proteins in each sample was confirmed by SDS-PAGE in parallel (right panel).

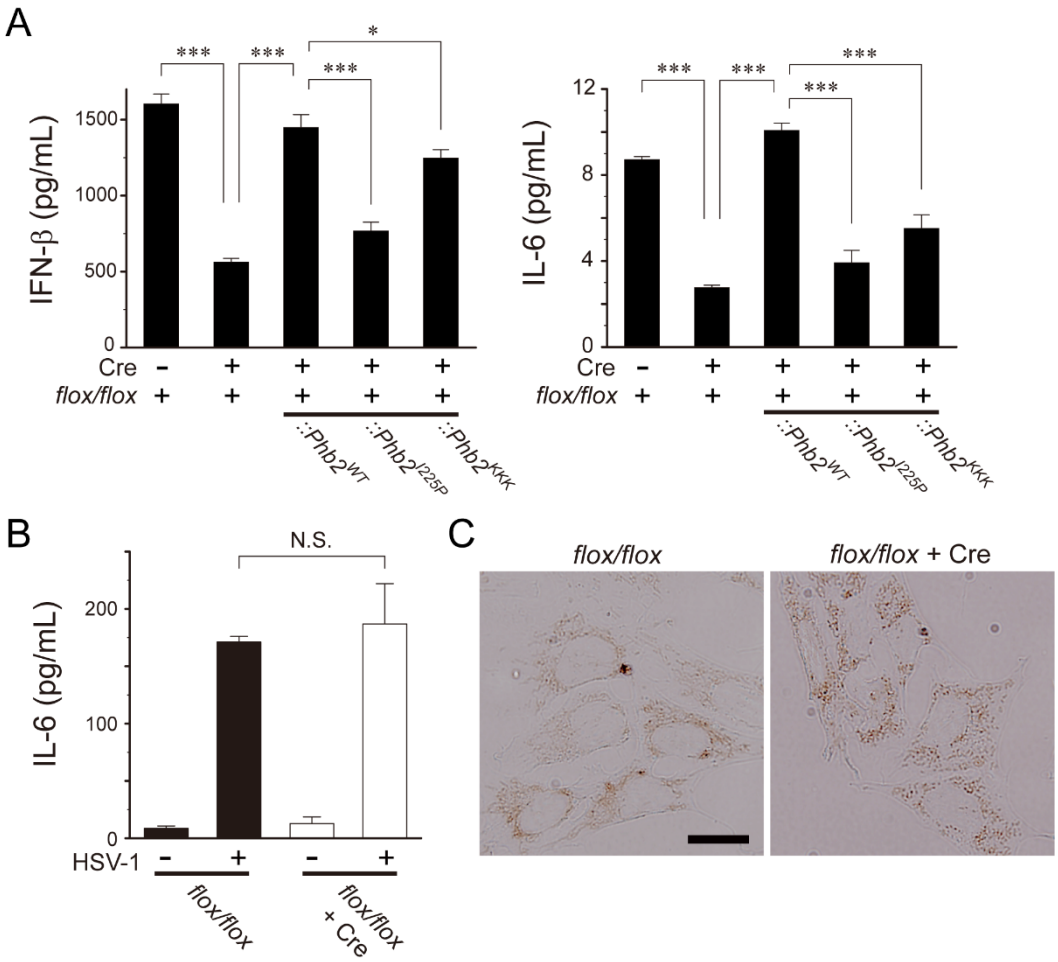


**Figure S3, related to Figure 3. Defective RIG-I pathway in *Phb2*-depleted cells**

(A) *Phb2*$^{flox/flox}$ and its variant MEFs were infected with SeV [4 hemagglutinin (HA) units/mL] for 18 h, and the cell-free supernatants were analyzed by ELISA to measure the amount of IFN-β (left) or IL-6 (right) secretion.

(B) *Phb2*$^{flox/flox}$ MEFs (± Cre) were infected with HSV-1 ($7 \times 10^4$ PFU) for 20 h, and the cell-free supernatants were analyzed by ELISA to measure the amount of IL-6 secretion. Each value represents the mean ± SEM (n = 3 experiments). Statistical analysis was performed using the two-tailed Student's *t* test. ***$p < 0.001$ and *$p < 0.05$, respectively. N.S., not significant.

(C) Comparison of COX activity between *Phb2*-depleted (+ Cre) and the control (left) MEFs. Cells expressing COX activity were indicated by a brown color. Scale bar, 20 μm.

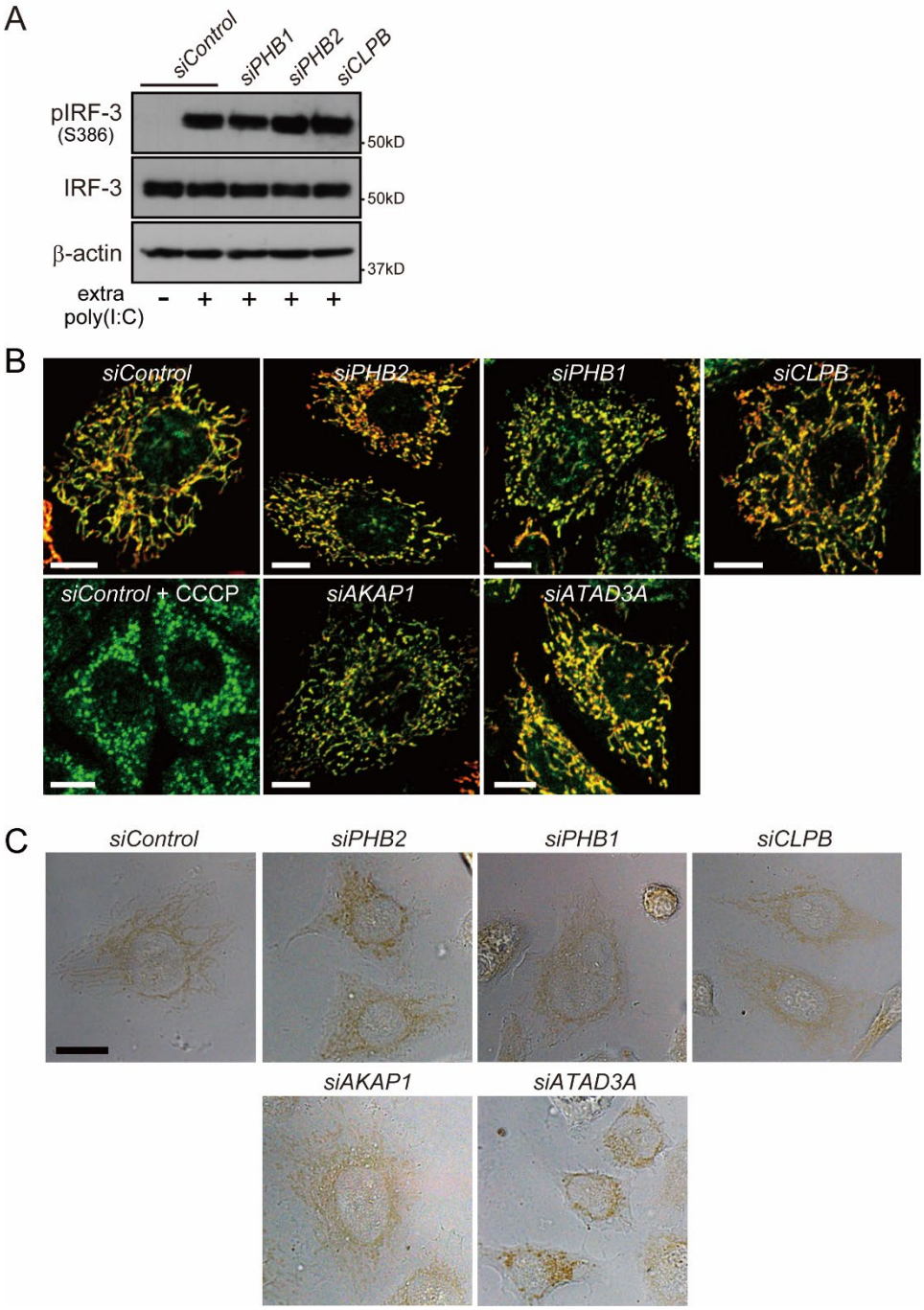


**Figure S4, related to Figure 5. Functionality of siRNA-treated cells**

(A) HEK293 cells stably expressing TLR-3 were treated with control or indicated siRNAs and the cells were stimulated with extracellular poly(I:C) (2 μg) for 16 h. Activation of endogenous IRF-3 was analyzed by Western blotting with antibody against phosphorylation of the $Ser^{386}$ site (pIRF-3). Anti-β-actin was used as the loading control.

(B) The siRNA-treated HeLa cells (as indicated) were stained with MitoTracker Red CMXRos,

which detects the mitochondrial membrane potential ($\Delta\Psi_m$), and mitochondria in the same cells were stained with an anti-COXIV monoclonal antibody (green). We confirmed that the siRNA-treated cells were uniformly detected with MitoTracker Red (highlighted in yellow), whereas CCCP-treated cells (bottom left panel) failed to stain with the dye, indicating loss of $\Delta\Psi_m$. Scale bar, 10 μm.

(C) Similar to (B), except that the COX activity of siRNA-treated cells was monitored. Cells expressing COX activity are indicated by the brown color. Scale bar, 20 μm.

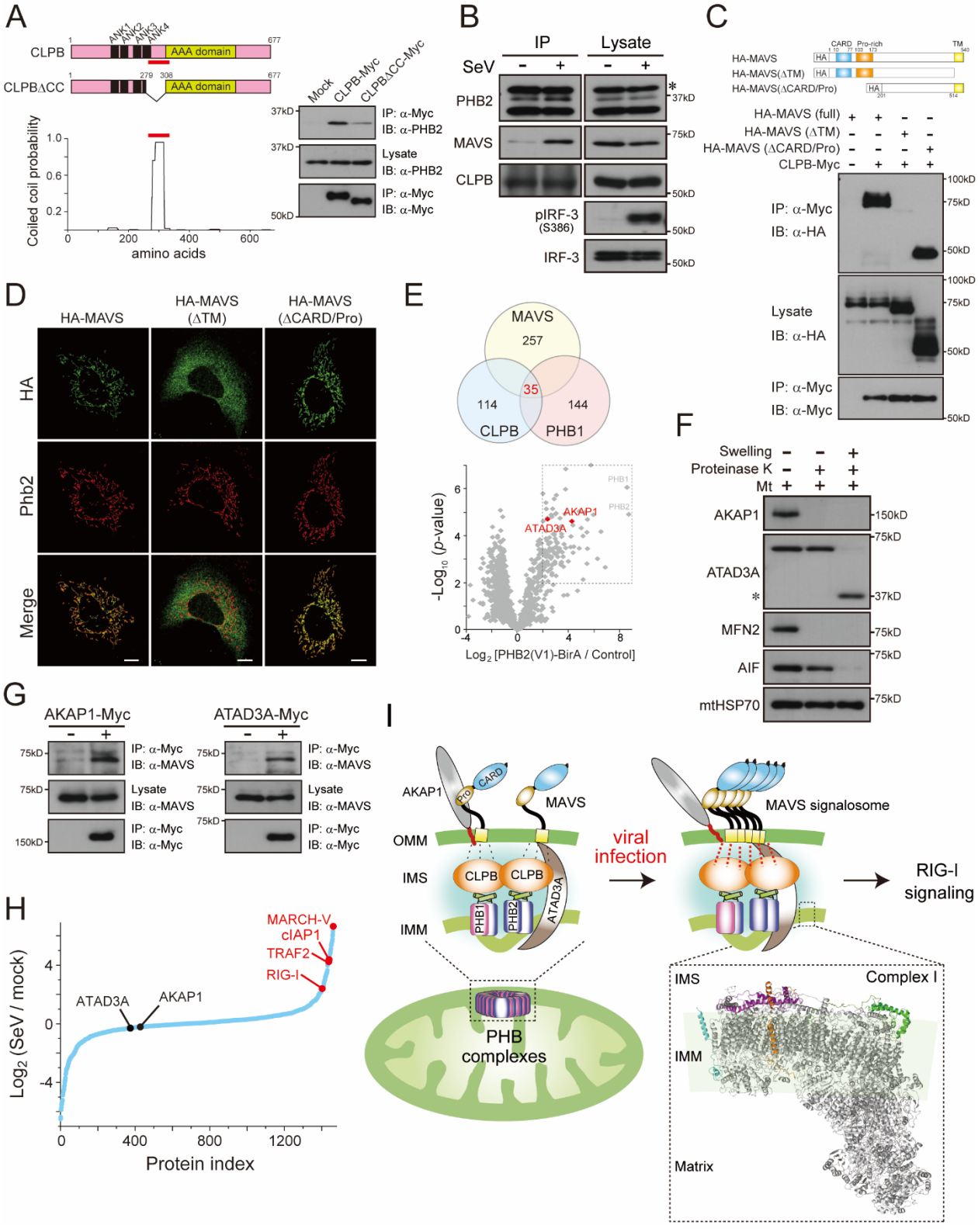
A
CLPB
CLPBΔCC
ANK1
ANK2
ANK3
ANK4
AAA domain
Coiled coil probability
amino acids
Mock
CLPB-Myc
CLPBΔCC-Myc
IP: α-Myc
IB: α-PHB2
Lysate
IB: α-PHB2
IP: α-Myc
IB: α-Myc
B
IP
Lysate
SeV
PHB2
MAVS
CLPB
pIRF-3
(S386)
IRF-3
C
HA-MAVS
HA-MAVS(ΔTM)
HA-MAVS(ΔCARD/Pro)
CARD
Pro-rich
TM
HA-MAVS (full)
HA-MAVS (ΔTM)
HA-MAVS (ΔCARD/Pro)
CLPB-Myc
IP: α-Myc
IB: α-HA
Lysate
IB: α-HA
IP: α-Myc
IB: α-Myc
D
HA-MAVS
HA-MAVS (ΔTM)
HA-MAVS (ΔCARD/Pro)
HA
Phb2
Merge
E
MAVS
257
35
114
144
CLPB
PHB1
-Log10 (p-value)
Log2 [PHB2(V1)-BirA / Control]
AKAP1
ATAD3A
F
Swelling
Proteinase K
Mt
AKAP1
ATAD3A
MFN2
AIF
mtHSP70
G
AKAP1-Myc
ATAD3A-Myc
IP: α-Myc
IB: α-MAVS
Lysate
IB: α-MAVS
IP: α-Myc
IB: α-Myc
H
Log2 (SeV / mock)
Protein index
MARCH-V
cIAP1
TRAF2
RIG-I
ATAD3A
AKAP1
I
AKAP1
CARD
Pro
MAVS
OMM
IMS
IMM
CLPB
PHB1
PHB2
ATAD3A
PHB complexes
viral infection
MAVS signalosome
RIG-I signaling
Complex I
Matrix

**Figure S5, related to Figure 5. Involvement of PHB complexes in antiviral innate immunity via CLPB with its binding partners**

(A) Interaction of endogenous PHB2 with CLPB. HEK293 cells were transfected with empty vector (Mock) or plasmids encoding the indicated CLPB constructs (top cartoon), and the lysates were subjected to immunoprecipitation (IP) with an anti-Myc antibody followed by analysis of Western blots with anti-PHB2 antibody. Graph at the bottom left shows the prediction results of the coiled-coil probability of CLPB using the program COILS.

(B) HEK293 cells stably expressing Myc-tagged PHB2 were mock-infected (-) or infected with SeV (4 HAU/mL) for 20 h, and postnuclear cell lysates were subjected to immunoprecipitation (IP) with the antibody against Myc followed by Western blot analysis with the antibody against MAVS. Asterisk indicates Myc-tagged PHB2.

(C) HEK293 cells stably expressing Myc-tagged CLPB were transfected with plasmids encoding HA-tagged MAVS variants, as indicated. Western blots of samples immunoprecipitated (IP) with the anti-Myc antibody or post-nuclear cell lysates (Lysate) were analyzed by immunoblotting (IB) with either the anti-HA monoclonal antibody HA.11 or the anti-Myc monoclonal antibody 9E10. The caspase recruitment domain (CARD), proline-rich domain (Pro-rich), and transmembrane segment (TM) in the MAVS structure are depicted (top cartoon), and the amino acid positions are indicated above the structure.

(D) The indicated HA-tagged MAVS variants in (C) were expressed in MEF cells, and their subcellular localizations were monitored by immunofluorescence against the HA antibody (green). Mitochondria in the same cells were identified by staining with an antibody against Phb2 (red). Scale bar, 10 μm.

(E) Identification of molecules that bridge the PHB complex to MAVS. Venn diagram in the top panel shows binding partners that overlapped (35 candidates) among the indicated molecules revealed by BioID2 assay (Table S5, abundance ratio > 7 for MAVS, and > 15 for both CLPB and PHB1). The volcano plot from Figure 1A is also shown at the bottom, and the positions of AKAP1 and ADAT3A are indicated in red.

(F) The mitochondrial fraction (Mt) isolated from HEK293 cells was treated with proteinase K (50 μg/mL) under regular (-) or hypotonic swelling (+) conditions for 15 min on ice. The reactants were developed by immunoblotting with antibodies against AKAP1, ATAD3A, or against several mitochondrial markers as indicated. OMM protein: MFN2. IMS protein: AIF. Matrix protein: mtHSP70. Asterisk indicates the C-terminal portion of ATAD3A.

(G) Interaction of endogenous MAVS with AKAP1 and ATAD3A. HEK293 cells were transfected with either AKAP1 (left) or ATAD3A (right) Myc-tagged encoding plasmids, and each lysate was subjected to immunoprecipitation (IP) with the anti-Myc antibody followed by Western blot analysis with anti-MAVS antibody.

(H) The interactions between AKAP1 and MAVS (also ATAD3A and MAVS) were not significantly altered during viral infection. A total of 1465 proteins identified from BioID2 experiments (BirA-MAVS ± SeV-infection) were plotted according to the abundance ratios ($log_2$) of SeV/mock against individual proteins (Protein index) sorted by their ratios in ascending order. Interactions, such as those of RIG-I and MAVS, were increased following the viral infection.
(I) Model of PHB complexes and their interactome that facilitates mitochondrial-mediated antiviral innate immunity. The PHB complexes localized in the IMM (left bottom) function in various mitochondrial homeostatic and cellular signaling processes. We propose that the PHB complexes comprising multi-oligomerizations of homotypic and/or heterotypic PHB dimers via their HR regions form an interactome assembly including CLPB, subunits of mitochondrial complex I, and other IMS proteins (left top, highlighted in blue background). Upon viral-infection, the PHB complexes associate with activated MAVS oligomers via CLPB with the assistance of proteins including AKAP1 and ATAD3A (middle), and the MAVS signalosome activates the RIG-I signaling pathway (right). These structural rearrangement events may be due to a functional role of CLPB, a molecular chaperone that responds to cellular stress. The right bottom inset shows the crystal structure of mitochondrial complex I (Zhu et al., 2016: PDB 5LC5), in which the specific subunits mentioned in the present study are colored in green (NDUFA8), cyan (NDUFB3), magenta (NDUFB10), and orange (NDUFB11).

**Table S3, related to Figure 2. Crystallographic data and refinement statistics**

| Diffraction data | |
|---|---|
| Resolution (last shell) (Å) | 46.06-1.70 (1.73-1.70) |
| Space group | $P4_122$ |
| Unit cell (Å) | 65.14, 65.14, 62.29 |
| Number of observed reflections | 172,229 (6,789) |
| Number of unique reflections | 15,289 (779) |
| Completeness (last shell) (%) | 99.8 (99.0) |
| $R_{merge}$ (%) | 5.1 (41.8) |
| $R_{meas}$ (last shell) (%) | 5.5 (46.7) |
| $I/\sigma(I)$ (last shell) | 22.3 (3.8) |
| $CC_{1/2}$ (%) | 100.0 (93.0) |

| Refinement statistics | |
|---|---|
| Resolution (Å) | 46.06-1.70 (1.83-1.70) |
| $R_{work}$ (%) | 21.6 (34.1) |
| $R_{free}$ (%) | 23.9 (35.2) |
| r.m.s.d. bonds (Å) | 0.008 |
| r.m.s.d. angles (deg) | 0.918 |
| Average B factor ($Å^2$) | 34.0 |
| Number of atoms (Protein) | 478 |
| Number of atoms (Water) | 75 |

# Transparent Methods

## Key Resources Table

| REAGENT or RESOURCE | SOURCE | IDENTIFIER |
|---|---|---|
| **Antibodies** | | |
| Mouse monoclonal anti-AIF (E-1) | Santa Cruz Biotechnology | sc-13116 |
| Rabbit monoclonal anti-AKAP1 (D9C5) | Cell Signaling Technology | Cat# 5203 |
| Mouse monoclonal anti-ATAD3A/B/C (A-4) | Santa Cruz Biotechnology | sc-376185 |
| Rabbit polyclonal anti-ATAD3A (C-term) | Jacques Baudier Laboratory | Gilquin B. et al., 2010 |
| Rabbit polyclonal anti-CLPB | Proteintech | 15743-1-AP |
| Rabbit monoclonal anti-Cre recombinase (D3U7F) | Cell Signaling Technology | Cat# 12830 |
| Rabbit monoclonal anti-CoxIV (3E11) | Cell Signaling Technology | Cat# 4850 |
| Rabbit polyclonal anti-cytochrome *c* (H-104) | Santa Cruz Biotechnology | sc-7159 |
| Rabbit polyclonal anti-HtrA2/Omi | R&D Systems | AF1458 |
| Mouse monoclonal anti-HA epitope tag (HA.11) | Covance | MMS-101P |
| Rat monoclonal anti-mouse-IL-6 | eBioscience | Cat# 14-7061-81 |
| Rabbit polyclonal anti-IRF-3 (FL-425) | Santa Cruz Biotechnology | sc-9082 |
| Rabbit monoclonal anti-IRF-3 (phospho S386) | Abcam | ab76493; EPR2346 |
| Rabbit polyclonal anti-MAVS | Abcam | ab25084 |
| Rabbit polyclonal anti-Mfn1 (H-65) | Santa Cruz Biotechnology | sc-50330 |
| Rabbit polyclonal anti-Mic19/CHCHD3 | Proteintech | 25625-1-AP |
| Mouse monoclonal anti-mtHsp70 | Thermo Fisher Scientific | MA3-028 |
| Mouse monoclonal anti-*c*-Myc epitope tag (9E10) | Covance | MMS-150P |
| Mouse monoclonal anti-OPA1 | BD Transduction Laboratories | Cat# 612606 |
| Mouse monoclonal anti-PGK1 (22C5D8) | Thermo Fisher Scientific | Cat# 459250 |
| Rabbit polyclonal anti-PHB2 (H-80) | Santa Cruz Biotechnology | sc-67045 |
| Rabbit monoclonal anti-PHB2/REA | Abcam | ab181838; EPR14522 |
| Rabbit monoclonal anti-PHB1 | Abcam | ab75766; EPR2803Y |
| Mouse monoclonal anti-Tim23 | BD Transduction Laboratories | Cat# 611223 |
| Mouse monoclonal anti-Tom20 (F-10) | Santa Cruz Biotechnology | sc-17764 |
| Rabbit polyclonal anti-Tom40 | Santa Cruz Biotechnology | sc-11414 |
| Alexa Fluor 488 goat anti-mouse IgG | Invitrogen | A-11001 |
| Alexa Fluor 568 goat anti-rabbit IgG | Invitrogen | A-11011 |
| Cy-3-conjugated sheep anti-mouse IgG | Jackson ImmunoResearch | Cat# 515-165-003 |
| **Bacterial and Virus Strains** | | |

| | | |
|---|---|---|
| *E. coli* BL21(DE3) competent cells | Novagen | Cat# 69450-3 |
| Sendai virus (Strain: Cantell) | ATCC | ATCC VR-907 |
| **Chemicals** | | |
| D-Biotin | Nacalai Tesque | Cat# 04822-04 |
| Digitonin | Wako Pure Chemical Industries | Cat# 043-21371 |
| Disuccinimidyl Dibutyric Urea (DSBU) | Thermo Fisher Scientific | Cat# A35459 |
| 3,3'-Diaminobenzidine | Tokyo Chemical Industry | D3756 |
| Isopropyl β-D-1-thiogalactopyranoside (IPTG) | Nacalai Tesque | Cat# 19742-94 |
| Lipofectamine 2000 | Thermo Fisher Scientific | Cat# 11668019 |
| Lipofectamine RNAiMAX | Thermo Fisher Scientific | Cat# 13778150 |
| Protease inhibitor cocktail | Roche | Cat# 11 836 153 001 |
| Phenylmethylsulfonyl fluoride (PMSF) | Nacalai Tesque | Cat# 06297-02 |
| poly(I:C) | InvivoGen | Cat# tlrl-pic |
| TRIzol | Invitrogen | Cat# 15596026 |
| Reverse Transcriptase (M-MLV) | Wako Pure Chemical Industries | Cat# 187-01281 |
| PrimeSTAR HS DNA Polymerase | Takara Bio | R010A |
| D-MEM, high glucose | Gibco | Cat# 11965092 |
| Bovine calf serum (BCS) | Gibco | Cat# 160170-078 |
| Fetal bovine serum (FBS) | Gibco | Cat# 10437028 |
| Penicillin-Streptomycin | Gibco | Cat# 15140122 |
| GlutaMAX | Gibco | Cat# 35050061 |
| Puromycin | Sigma-Aldrich | P8833 |
| Blasticidin | InvivoGen | Cat# ant-bl-05 |
| Hygromycin B | Sigma-Aldrich | H3274 |
| G-418 (Geneticin) | Roche | Cat# 04 727 878 001 |
| MitoTracker Red CMXRos | Invitrogen | M7512 |
| Anti-c-Myc Agarose beads | Sigma-Aldrich | A7470 |
| Streptavidin Agarose beads | Sigma-Aldrich | S1638 |
| Protein A Sepharose beads | Sigma-Aldrich | P3391 |
| Nickel-nitriotriacetate (Ni-NTA) agarose | QIAGEN | Cat# 30210 |
| HiTrap Q HP | GE Healthcare | Cat# 17115301 |
| **Critical Commercial Assays** | | |
| Human IFN-β ELISA Kit | Kamakura Techno-Science | Cat# KTS301 |

| | | |
|---|---|---|
| Mouse IFN-β ELISA Kit | R&D Systems | Cat# 42400-1 |
| Dual-Luciferase reporter assay system | Promega | E1910 |
| **Deposited Data** | | |
| $PHB2^{188-265}$ crystal structure | This paper | PDB: 6IQE |
| BioID2 data [Control, PHB2(V1), PHB2(V3)] | This paper | jPOST: PXD011939 |
| BioID2 data ($PHB2^{WT}$, $PHB2^{I225P}$, $PHB2^{KKK}$) | This paper | jPOST: PXD011946 |
| BioID2 data (MAVS, CLPB, PHB1) | This paper | jPOST: PXD014218 |
| Cross-linking MS data | This paper | jPOST: PXD011941 and PXD014217 |
| **Experimental Models: Cell Lines** | | |
| HEK293 | Tsurimoto Laboratory | N/A |
| A549 | Ichinohe Laboratory | N/A |
| HeLa | Mihara Laboratory | N/A |
| *Phb2*$^{flox/flox}$ MEFs | Thomas Langer Laboratory | N/A |
| Platinum-A retroviral packaging cell line | Cell Biolabs | RV-102 |
| **Experimental Models: Yeast strains** | | |
| Wild Type (TKY705) (genetic background W303): *MAT*a *ura3-52 trp1*Δ *leu2-3_112 his3-11 ade2-1* | Miyata N. et al., 2017 | N/A |
| Wild Type (TKY706) (genetic background W303): *MAT*α *ura3-52 trp1*Δ *leu2-3_112 his3-11 ade2-1 can1* Δ *::STE2pr-Sp_his5* | Miyata N. et al., 2017 | N/A |
| *psd*1Δ (TKY707): TKY705, *psd1*Δ::*kanMX4* | Miyata N. et al., 2017 | N/A |
| *phb1*Δ (OKY7207): TKY706, *phb1*Δ*::hphNT1* | This paper | N/A |
| *PSD1/psd1*Δ *PHB1/phb1*Δ (OKY7208) (genetic background W303): *MAT*a/α *ura3-52/ura3-52 trp1*Δ*/ trp1*Δ *leu2-3_112/ leu2-3_112 his3-11/his3-11 ade2-1/ade2-1 CAN1/can1* Δ *::STE2pr-Sp_his5 PSD1/psd1*Δ::*kanMX4 PHB1/phb1* Δ*::hphNT1* | This paper | N/A |
| **Oligonucleotides** | | |
| Human PHB2 (A.A.1) forward (TK1090): 5'-aaagctagcgtttaaaccatggcccagaacttgaaggacttgg | FASMAC | N/A |
| Human PHB2 (A.A.299) reverse (TK1091): 5'-tttgaattctttcttacccttgatgaggc | FASMAC | N/A |
| Human PHB2 (A.A.188) forward (TK1028): 5'-tttaccatggggagctttagccgagagtacacagc-3' | FASMAC | N/A |
| Human PHB2 (A.A.247) reverse (TK1029): 5'-tttctcgaggccagggttcttgctcagtgc-3' | FASMAC | N/A |
| Human PHB2 (I225P) mutation forward: 5'-cggcagaaaCCtgtgcaggccgag-3' | FASMAC | N/A |
| Human PHB2 (I225P) mutation reverse: 5'-ctcggcctgcacaGGtttctgccg-3' | FASMAC | N/A |
| Human PHB2 (KKK) mutation forward: 5'-gcaggccAagggtAaggccAaggctgcc-3' | FASMAC | N/A |

| | | |
|---|---|---|
| Human PHB2 (KKK) mutation reverse:<br>5'-ggcagcctTggcctTaccctTggcctgc-3' | FASMAC | N/A |
| Human CLPB (A.A.1) forward:<br>5'-aaagctagcaccatgctggggtccctggtgttgaggagaaaagc-3' | FASMAC | N/A |
| Human CLPB (A.A.677) reverse:<br>5'-tttggtaccgatggtgttgcacaccttctcagggtgcagtgg-3' | FASMAC | N/A |
| Human CLPB (Δ A.A.280-307) deletion forward:<br>5'-ggattatgcccgagaagggcccctggagcagcgactaaagg-3' | FASMAC | N/A |
| Human CLPB (Δ A.A.280-307) deletion reverse:<br>5'-cctttagtcgctgctccaggggcccttctcgggcataatcc-3' | FASMAC | N/A |
| Human AKAP1 (A.A. 1) forward:<br>5'-aaagcggccgcaccatggcaatccagttccgttcgctcttcccc-3' | FASMAC | N/A |
| Human AKAP1 (A.A. 903) reverse:<br>5'-tttggtaccaaggcttgtgtagtagctgtctacccactgg-3' | FASMAC | N/A |
| Human ATAD3A (A.A. 1) forward:<br>5'-aaagctagcaccatgtcgtggctcttcggcattaacaagggc-3' | FASMAC | N/A |
| Human ATAD3A (A.A. 634) reverse:<br>5'-tttggtaccggatggggagggctcgtccccacgc-3' | FASMAC | N/A |
| *S. cerevisiae* genomic DNA (*Phb1* ORF) forward:<br>5'-aaactcgagggtaggggttcgctatggggtcatcactggcc-3' | FASMAC | N/A |
| *S. cerevisiae* genomic DNA (*Phb1* ORF) reverse:<br>5'-tttggatccgcagccaccgctttggctgtaggtataagatgcc-3' | FASMAC | N/A |
| *S. cerevisiae Phb1*-Myc tag (A.A. 287) forward:<br>5'-agtggagaacaaaagttgatttctgaagaagatttgtaagtctggaaaagctatgaacacaataaactag-3' | FASMAC | N/A |
| *S. cerevisiae Phb1*-Myc tag (A.A. 287) reverse:<br>5'-ttacaaatcttcttcagaaatcaacttttgttctccactacggccaatgttcaaaagcaaggaatttgg-3' | FASMAC | N/A |
| *S. cerevisiae Phb1* (V202P) mutation forward:<br>5'-gccaaattccttCCcgaaaaggcagagc-3' | FASMAC | N/A |
| *S. cerevisiae Phb1* (V202P) mutation reverse:<br>5'-gctctgccttttcgGGaaggaatttggc-3' | FASMAC | N/A |
| *S. cerevisiae Phb1* (V213P) mutation forward:<br>5'-gagacaagcttctCCtatcagagctgaagg-3' | FASMAC | N/A |
| *S. cerevisiae Phb1* (V213P) mutation reverse:<br>5'-ccttcagctctgataGGagaagcttgtctc-3' | FASMAC | N/A |
| *S. cerevisiae Phb1* (KKK) mutation forward:<br>5'-gttatcagagctAaaggtAaagcaAaaagtgctgaattc-3' | FASMAC | N/A |
| *S. cerevisiae Phb1* (KKK) mutation reverse:<br>5'-gaattcagcactttTtgcttTaccttTagctctgataac-3' | FASMAC | N/A |
| *S. cerevisiae Phb1* disruption forward:<br>5'-acgaaacttacattcaaaatcaataatttactttagaaaagaatgcgtatgcaggtcgac-3' | Sigma-Aldrich | N/A |
| *S. cerevisiae Phb1* disruption reverse:<br>5'-aattttctcccctagtttattgtgttcatagcttttccagacttaatcgatgaattcgagctcg-3' | Sigma-Aldrich | N/A |
| **siRNA** | | |
| *AKAP1 Sense siRNA sequence*<br>*UCAACAUCAUGUAGACAAAtt* | Thermo Fisher Scientific | s15665 |
| *ATAD3A Sense siRNA sequence*<br>*UGGUGAGAAUGUAUUUUGAtt* | Thermo Fisher Scientific | s30448 |
| *CCDC58 Sense siRNA sequence #1*<br>*AGUCUUUGAUGGCAGCUCAtt* | Thermo Fisher Scientific | s228144 |

| | | |
|---|---|---|
| *CCDC58 Sense siRNA sequence #2 AGAACUGAAUGUUGAAGAAtt* | Thermo Fisher Scientific | s43575 |
| *CCDC58 Sense siRNA sequence #3 CAGACAAAGUUGAAAUGGAtt* | Thermo Fisher Scientific | s43576 |
| *CMC2 Sense siRNA sequence #1 GGUUGAUACCUGAAAGAAUtt* | Thermo Fisher Scientific | s226898 |
| *CMC2 Sense siRNA sequence #2 GCAUUGCAAUGCGAAAGAAtt* | Thermo Fisher Scientific | s32444 |
| *CMC2 Sense siRNA sequence #3 GAUCGGGAGUUGAGAAAAUtt* | Thermo Fisher Scientific | s32446 |
| *DIABLO Sense siRNA sequence #1 GACUGCAGUUGGUCUUUCAtt* | Thermo Fisher Scientific | s32189 |
| *DIABLO Sense siRNA sequence #2 CCGACAAUAUACAAGUUUAtt* | Thermo Fisher Scientific | s32187 |
| *DIABLO Sense siRNA sequence #3 UCUCUUUACCGACAAUAUAtt* | Thermo Fisher Scientific | s32188 |
| *PGAM5 Sense siRNA sequence #1 AGCUGUGCAGUAUUACGAAtt* | Thermo Fisher Scientific | s46938 |
| *PGAM5 Sense siRNA sequence #2 GCAGUAUUACGAAGACGGAtt* | Thermo Fisher Scientific | s46937 |
| *PGAM5 Sense siRNA sequence #3 CCAGGCGUCUGCAAAGUCAtt* | Thermo Fisher Scientific | s195818 |
| *NDUFB11 Sense siRNA sequence #1 GCGACUUGUCUUCUUCUUUtt* | Thermo Fisher Scientific | s224300 |
| *NDUFB11 Sense siRNA sequence #2 CGUGGGAUGGGAUGAAAGAtt* | Thermo Fisher Scientific | s29163 |
| *NDUFB11 Sense siRNA sequence #3 CCGAGGACGAAAACUUGUAtt* | Thermo Fisher Scientific | s29165 |
| *CLPB Sense siRNA sequence #1 GGAUCAUCUGGAAUAGGAAtt* | Thermo Fisher Scientific | s224882 |
| *CLPB Sense siRNA sequence #2 GGAAGACCAUUGAUUGCAAtt* | Thermo Fisher Scientific | s37653 |
| *CLPB Sense siRNA sequence #3 GCUUUGGAGAUGAGCCGUAtt* | Thermo Fisher Scientific | s37655 |
| *NDUFB3 Sense siRNA sequence #1 CUGCAUUUGUGGUAGCUGUtt* | Thermo Fisher Scientific | s9355 |
| *NDUFB3 Sense siRNA sequence #2 ACUUCCAGAUUAUAGACAAtt* | Thermo Fisher Scientific | s9356 |
| *NDUFB3 Sense siRNA sequence #3 AGAUAGAAGGGACACCAUUtt* | Thermo Fisher Scientific | s9357 |
| *CKMT1B Sense siRNA sequence #1 GCACACCACGGAUCUAGAUtt* | Thermo Fisher Scientific | s3097 |
| *CKMT1B Sense siRNA sequence #2 AGGUAUGUAUUGUCCUCUAtt* | Thermo Fisher Scientific | s3099 |
| *CKMT1B Sense siRNA sequence #3 GUAUUGUCCUCUAGAGUCAtt* | Thermo Fisher Scientific | s3098 |
| *NDUFA8 Sense siRNA sequence #1 GCAGUUAUUUCGUCACUGUtt* | Thermo Fisher Scientific | s9342 |
| *NDUFA8 Sense siRNA sequence #2 GGAGAACUGUCAAAGGUCAtt* | Thermo Fisher Scientific | s9340 |
| *NDUFA8 Sense siRNA sequence #3 GGACUUCUUUAGGCAGAUAtt* | Thermo Fisher Scientific | s9341 |

| | | |
|---|---|---|
| *IMMP2L Sense siRNA sequence #1 AGAGAGUGAUUGCUCUUGAtt* | Thermo Fisher Scientific | s38358 |
| *IMMP2L Sense siRNA sequence #2 GGGUUGAAGGUGAUCAUCAtt* | Thermo Fisher Scientific | s38357 |
| *IMMP2L Sense siRNA sequence #3 GUGGUGACAUUGUAUCAUUtt* | Thermo Fisher Scientific | s38356 |
| *NDUFB10 Sense siRNA sequence #1 GGACUACAAAGUCGACCAAtt* | Thermo Fisher Scientific | s9375 |
| *NDUFB10 Sense siRNA sequence #2 GUGCAUGUAUGAAGCCGAAtt* | Thermo Fisher Scientific | s9376 |
| *NDUFB10 Sense siRNA sequence #3 GCAGAACUGUAUCAAGGAAtt* | Thermo Fisher Scientific | s9374 |
| *PHB1 Sense siRNA sequence #1 UCACAACUGAGAUCCUCAAtt* | Thermo Fisher Scientific | s10426 |
| *PHB1 Sense siRNA sequence #2 CGUGGGUACAGAAACCAAUtt* | Thermo Fisher Scientific | s10424 |
| *PHB1 Sense siRNA sequence #3 GCAUCGGAGAGGACUAUGAtt* | Thermo Fisher Scientific | s10425 |
| Silencer Select Negative Control No. 1 *siRNA* | Thermo Fisher Scientific | Cat# 4390843 |
| **Recombinant DNA** | | |
| Plasmid: pET28a/PHB2$^{188\text{-}247}$-6×His | This study | N/A |
| Plasmid: pET28a/PHB2$^{188\text{-}247}$(I225P)-6×His | This study | N/A |
| Plasmid: pET28a/PHB2$^{188\text{-}247}$(KKK)-6×His | This study | N/A |
| Plasmid: pET28a/PHB2$^{188\text{-}265}$-6×His | This study | N/A |
| Plasmid: pcDNA3.1(-)/C terminal-3×Myc tag | Yasukawa K. et al., 2009 | N/A |
| Plasmid: pcDNA3.1(-)/PHB2-3×Myc | This study | N/A |
| Plasmid: pcDNA3.1(-)/PHB2$^{I225P}$-3×Myc | This study | N/A |
| Plasmid: pcDNA3.1(-)/PHB2$^{KKK}$-3×Myc | This study | N/A |
| Plasmid: pcDNA3.1(-)/CLPB-3×Myc | This study | N/A |
| Plasmid: pcDNA3.1(-)/CLPB$^{\Delta 280\text{-}307}$-3×Myc | This study | N/A |
| Plasmid: pcDNA3.1(-)/AKAP1-3×Myc | This study | N/A |
| Plasmid: pcDNA3.1/ATAD3A-myc-6×His | Gilquin B. et al., 2010 | N/A |
| Plasmid: MCS-BioID2-HA | Addgene (Kyle Roux Lab) | Cat# 74224 |
| Plasmid: pcDNA3.1/PHB2(V1)-BirA-HA | This study | N/A |
| Plasmid: pcDNA3.1/PHB2(V3)-BirA-HA | This study | N/A |
| Plasmid: pcDNA3.1/PHB2 $^{I225P}$ -BirA-HA | This study | N/A |
| Plasmid: pcDNA3.1/PHB2 $^{KKK}$ -BirA-HA | This study | N/A |
| Plasmid: pcDNA3.1/PHB1-BirA-HA | This study | N/A |
| Plasmid: pcDNA3.1/CLPB-BirA-HA | This study | N/A |

| | | |
|---|---|---|
| Plasmid: pMXs-puro | Cell Biolabs | RTV-012 |
| Plasmid: pMXs-puro/PHB2-3×Myc | This study | N/A |
| Plasmid: pMXs-puro/PHB2$^{I225P}$-3×Myc | This study | N/A |
| Plasmid: pMXs-puro/PHB2$^{KKK}$-3×Myc | This study | N/A |
| Plasmid: pMXs-puro/PHB2(V1)-BirA-HA | This study | N/A |
| Plasmid: pMXs-puro/PHB2(V3)-BirA-HA | This study | N/A |
| Plasmid: pMXs-puro/NLS-Cre | This study | N/A |
| Plasmid: pMXs-puro/NLS-Cre-eGFP | This study | N/A |
| Plasmid: pMXs-puro/CLPB-3×Myc | This study | N/A |
| Plasmid: myc-BioID2-MCS | Addgene (Kyle Roux Lab) | Cat# 74223 |
| Plasmid: pcDNA3.1/myc-BirA-MAVS$^{1-540}$ | This study | N/A |
| Plasmid: pcDNA3.1(-)/3×Myc-MAVS$^{1-540}$ | Yasukawa K. et al., 2009 | N/A |
| Plasmid: pcDNA3.1(-)/3×HA-MAVS$^{1-540}$ | Yasukawa K. et al., 2009 | N/A |
| Plasmid: pcDNA3.1(-)/3×HA-MAVS$^{1-514}$ | Yasukawa K. et al., 2009 | N/A |
| Plasmid: pcDNA3.1(-)/3×HA-MAVS$^{201-540}$ | Yasukawa K. et al., 2009 | N/A |
| Plasmid: pcDNA3.1(-)/RIG-I$^{1-250}$-7×Myc | Yasukawa K. et al., 2009 | N/A |
| Plasmid: pRS416 | ATCC | ATCC 87521 |
| Plasmid: pRS416/yPhb1$^{WT}$-Myc | This study | N/A |
| Plasmid: pRS416/yPhb1$^{V202P}$-Myc | This study | N/A |
| Plasmid: pRS416/yPhb1$^{V213P}$-Myc | This study | N/A |
| Plasmid: pRS416/yPhb1$^{V202/213P}$-Myc | This study | N/A |
| Plasmid: pRS416/yPhb1$^{KKK}$-Myc | This study | N/A |
| **Software and Algorithms** | | |
| COILS | Lupas A. et al., 1991 | https://embnet.vital-it.ch/software/COILS_form.html |
| GraphPad QuickCalcs | GraphPad Software | https://www.graphpad.com/quickcalcs/ttest1.cfm |
| PyMOL version 2.1.1 | The PyMOL Molecular Graphics System, Version 2.0 Schrödinger, LLC | https://pymol.org/2 |
| Proteome Discoverer version 2.2 | Thermo Fisher Scientific | OPTON-30795 |
| CCP4 6.4.0 | Winn M.D. et al., 2011 | http://www.ccp4.ac.uk/index.php |

| | | |
|---|---|---|
| Xds version May 1, 2016 | Kabsch W., 2010 | http://xds.mpimf-heidelberg.mpg.de/ |
| Phenix version 1.8.4-1496 | Adams P.D. et al., 2010 | https://www.phenix-online.org/ |
| Coot 0.7.2 | Emsley P. et al., 2010 | https://www2.mrc-lmb.cam.ac.uk/personal/pemsley/coot/ |

**Cell lines and virus**

HEK293 cells (obtained from the Tsurimoto Laboratory, species: human, sex: female) were maintained in Dulbecco's modified Eagle medium (D-MEM) (high glucose; 4,500 mg/L) supplemented with 1% GlutaMAX, penicillin (100 U/mL)-streptomycin (100 μg/mL), and 10% bovine calf serum (BCS) at 5% $CO_2$ and 37° C. A549 (obtained from the Ichinohe Laboratory, species: human, sex: male), HeLa (obtained from the Mihara Laboratory, species: human, sex: female), and *Phb2*$^{flox/flox}$ MEFs (obtained from the Langer Laboratory, species: mouse, sex: unknown) were maintained in D-MEM medium supplemented with 1% GlutaMAX, penicillin (100 U/mL)-streptomycin (100 μg/mL), and 10% fetal bovine serum (FBS) at 5% $CO_2$ and 37° C. The Platinum-A retroviral packaging cell line (obtained from Cell Biolabs: human, sex: unknown) was similarly maintained in D-MEM/FBS medium, except with the addition of puromycin (1 μg/mL) and blasticidin (10 μg/mL). Cells used in the study were authenticated via a Short Tandem Repeat analysis. Sendai virus Cantell strain used in the study was purchased from the American Type Culture Collection (ATCC).

**Yeast strains and their genotyping**

The yeast strains were grown in YPAD medium (pH 6.0) containing 1% yeast extract, 2% peptone, 0.008% adenine, and 2% glucose. Synthetic complete medium plus adenine (SCAD medium, pH 6.0) containing 0.67% yeast nitrogen base without amino acids, 0.2% drop-out mix, 0.008% adenine, and 2% glucose without uracil was used for selecting the uracil-prototrophic transformants. SCAD-MSG medium (pH 6.0) containing 0.17% yeast nitrogen base without amino acids and ammonium sulfate, 0.1% *L*-glutamic acid sodium salt, 0.2% drop-out mix, 0.008% adenine, and 2% glucose, without histidine and uracil was used for random spore analyses (Tong and Boone, 2006). Complete disruption of the *phb1* gene was accomplished by polymerase chain reaction (PCR)-based gene replacement (Lorenz et al., 1995) using a hygromycin-resitant cassette amplified from a plasmid pFA6a-hphNT1 (Janke et al., 2004) with a pair of gene-specific primers (PHB1 disruption forward/reverse oligonucleotides in the Key Resources Table). A diploid yeast strain, *PSD1*/*psd1*Δ *PHB1*/*phb1*Δ (OKY7208), was obtained by mating a *MATa* strain, *psd1*Δ::*kanMX4* and a *MAT*α strain, *phb1*Δ::*hphNT1*, followed by incubation on a diploid selection agar-plate containing YPD medium supplemented with 200 μg/mL of G-418 and 300 μg/mL of hygromycin B.

**Plasmids**

To construct human PHB2 (variants 1 and 3) plasmids used in the BioID2 study, HEK293 cDNA was used as a template for PCR to amplify the gene. Using the oligonucleotides TK1090 and TK1091, each amplified fragment containing 5' *Nhe*I and 3' *EcoR*I sites was subcloned into a plasmid (MCS-BioID2-HA; Addgene #74224) containing a carboxyl-terminal HA epitope tag with a biotin ligase from *Aquifex aeolicus*. To generate PHB2 bacterial expression constructs, the plasmid pcDNA3.1/PHB2(V1)-BirA-HA was used as a template to PCR-amplify regions encoding residues 188–247 (coiled-coil motif) with a forward primer (TK1028) containing a 5' *Nco*I restriction site and a reverse primer (TK1029) containing a 3' *Xho*I site. The amplified fragment was ligated into pET28a (+) (Novagen), which contains a C-terminal 6×His tag. The human CLPB, AKAP1, and ATAD3A-encoding genes were obtained from HEK293 cells, and the cDNAs were each subcloned into a pcDNA3.1(-)/3×Myc vector in-frame with 3×Myc tag (Yasukawa et al., 2009). To construct pRS416/yPhb1-Myc, a yeast centromere plasmid carrying *Phb1*, a genomic fragment containing the *Phb1*-coding region with 500 bp of the 5′ and 3′ flanking sequences was amplified by PCR from the *S. cerevisiae* genomic DNA of *MATα* strain using primer sets of *Phb1 ORF* forward and reverse, and then cloned into pRS416 (ATCC 87521) in-frame with a Myc epitope tag. Mutations of each plasmid used in the study were introduced by overlap PCR mutagenesis and confirmed by DNA sequencing (ABI 3100). To generate retroviral expression constructs, each cDNA was subcloned into the retroviral vector pMXs-puro (Cell Biolabs). The retroviral expression vectors were then transfected into platinum packaging cell lines by calcium phosphate precipitation, and the retroviral supernatants were harvested 48 h post-transfection and used to infect cells. The plasmid encoding Cre recombinase fused with a nuclear localization signal (NLS) was obtained from Addgene (#13763).

**Protein expression and purification**

PHB2$^{188\text{-}247}$ (or PHB2$^{188\text{-}265}$) with a C-terminal 6×His tag and its variants were expressed in *E. coli* BL21(DE3) cells. Inoculated cultures were grown to log phase at 37° C. Overproduction of recombinant protein was induced by the addition of isopropyl β-D-1-thiogalactopyranoside to a final concentration of 1 mM at 15° C for overnight induction. The next day, cells were collected by centrifugation (6,700*g* for 15 min), and the pellets were stored frozen (-20° C) until purification. Bacterial pellets were resuspended in 50 mM Tris-buffered saline (pH 8.0) containing 300 mM NaCl, 10% glycerol (w/v), 15 mM imidazole, and 1 mM phenylmethylsulfonyl fluoride (PMSF), lysed by sonication, and centrifuged at 18,800*g* at 4° C for 15 min to obtain a soluble fraction. After clarification, the histidine-tagged

proteins were affinity-purified on nickel-nitriotriacetate (Ni-NTA) agarose columns at 4° C. Proteins bound to the beads were eluted with 50 mM Tris-HCl buffer (pH 8.0) containing 300 mM NaCl and 100 mM imidazole. After elution, all proteins were purified to >95% purity by anion exchange chromatography using a HiTrapQ column equilibrated with 50 mM Tris-HCl buffer (pH 8.5). Protein concentrations were determined by absorbance at 280 nm in 6M guanidine hydrochloride (Edelhoch 1967).

**Circular dichroism spectroscopy**

CD measurements were performed in 1× phosphate-buffer saline (PBS; pH 7.4) with a Jasco J-715 spectropolarimeter (JASCO Co). Wavelength scans (200 to 250 nm) were performed on 10 μM protein solutions using a cell with 0.2 cm optical path length at 4° C.

**Crystallization, X-ray data collection, and structure determination**

Crystallizations were performed using the histidine-tagged PHB2$^{188\text{-}265}$ protein. Diffraction-quality crystals of PHB2$^{188\text{-}265}$ were obtained by vapor diffusion of hanging drops at 20° C by equilibrating protein against a reservoir solution containing 1.0 M ammonium chloride and 0.1 M sodium acetate (pH 4.5). Bipyramidal crystals belonged to the space group $P4_122$ ($a = b = 65.14$ Å, $c = 62.29$ Å). Crystals were soaked into a cryoprotectant solution containing 1.1 M ammonium chloride, 0.1 M sodium acetate (pH 4.5), and 20% (w/v) glycerol, and flash-frozen in liquid nitrogen for synchrotron data collection.

The X-ray diffraction data of the PHB2$^{188\text{-}265}$ crystals were collected from a single crystal at 100K on a PILATUS 6M pixel detector (Dectris) using a single wavelength (1.0000 Å) at beamline BL41XU at SPring-8, Japan. Integrated intensities were obtained with the program XDS and scaled using the program AIMLESS in the CCP4 package. The initial model of the PHB2$^{188\text{-}265}$ was obtained by molecular replacement using the program PHASER. The search model was a monomer in a computationally designed three-helix bundle (PDB ID: 4TQL). Structural refinement was performed using phenix.refine from the PHENIX suite. In the final refined structure, only residues 188-245 were ordered. The crystal structure contained 76 water molecules. The refined coordinate for PHB2$^{188\text{-}265}$ was deposited in the Protein Data Bank (PDB ID: 6IQE). Data processing and crystallographic refinement statistics are summarized in Table S3.

**Mitochondrial fractionation and proteolysis**

Mitochondrial fractionation, proteolysis and membrane association assays were performed as previously described (Yoshizumi et al. 2014) with slight modifications. Briefly, cultured cells were washed once with 1× PBS (pH 7.4), scraped off the culture plate, and lysed in

homogenization buffer containing 20 mM HEPES (pH 7.5), 70 mM sucrose, and 220 mM mannitol by 30 strokes in a Dounce homogenizer. The homogenate was then centrifuged at 800*g* for 5 min (4° C) to precipitate the nuclei, and the resulting supernatant was further centrifuged at 10,000*g* for 10 min (4° C) to precipitate the crude mitochondrial fraction.

For the proteinase K resistance assay, the isolated mitochondria pellet was resuspended in either the homogenization buffer or a hypotonic buffer [20 mM HEPES (pH 7.5)] and maintained on ice for 30 min to cause swelling. The samples were then treated with proteinase K (50 μg/mL) for 15 min (on ice), and reactants were subjected to Western blot analysis with the indicated antibodies.

**Blue-Native PAGE**

The isolated mitochondrial fraction was lysed in a BN-PAGE lysis buffer containing 20 mM Bis-Tris (pH 7.0), 2 mM NaCl, 500 mM aminocaproic acid, 1 mM EDTA, 10% (v/v) glycerol, 0.5% (w/v) digitonin, and protease inhibitor cocktail on ice for 15 min. The clarified supernatant was supplemented with 0.5% (w/v) Coomassie brilliant blue G-250, separated on 4-12% BN-PAGE, and immunoblotted with the indicated antibodies.

**The proximity-dependent biotin identification (BioID2)**

The proximity-dependent biotin identification (BioID2) method was performed as previously described (Kim et al. 2016) with slight modifications. Briefly, confluent HEK293 cells in 10-cm dish that stably expressed PHB2(V1 or V3) or other proteins fused at the C-terminus with the biotin ligase from *A. aeolicus* were incubated with 100 μM biotin for 18 h. After washing once with 1× PBS (pH 7.4), the cells were scraped off and mitochondria from the cells were isolated as described above. The mitochondrial fractions were then washed once with the homogenization buffer and lysed in 800 μL radio immunoprecipitation assay (RIPA) buffer containing 50 mM Tris-HCl (pH 7.4), 150 mM NaCl, 1 mM EDTA-EGTA, 10% (w/v) glycerol, 1% (w/v) Nonidet P-40 (NP-40), 0.1% sodium dodecyl sulfate (SDS), and 0.1% sodium deoxycholate for 1 h at 4° C. The clarified supernatants were incubated with 20 μL of streptavidin agarose beads for 2 h at 4° C, followed by washing three times with RIPA buffer and twice with 50 mM ammonium bicarbonate. Proteins on the beads were digested by adding 200 ng trypsin/Lys-C mix (Promega) for 16 h at 37° C. The digests were desalted using GL-Tip SDB (GL Sciences), and the eluates were evaporated in a SpeedVac concentrator (Thermo Fisher Scientific).

LC-MS/MS analysis of the resultant peptides was performed on an EASY-nLC 1200 UHPLC connected to a Q Exactive Plus mass spectrometer through a nanoelectrospray ion source (Thermo Fisher Scientific). The peptides were separated on a 75-μm inner diameter × 150 mm

C18 reverse-phase column (Nikkyo Technos) with a linear gradient from 4%-28% acetonitrile for 0-150 min followed by an increase to 80% acetonitrile during 150-170 min. The mass spectrometer was operated in a data-dependent acquisition mode with a top 10 MS/MS method. MS1 spectra were measured with a resolution of 70,000, an AGC target of $1 \times 10^6$, and a mass range from 350 to 1,500 *m/z*. HCD MS/MS spectra were acquired at a resolution of 17,500, an AGC target of $5 \times 10^4$, an isolation window of 2.0 *m/z*, a maximum injection time of 60 ms, and a normalized collision energy of 27. Dynamic exclusion was set to 10 s. Raw data were directly analyzed against the SwissProt database restricted to *Homo sapiens* using Proteome Discoverer version 2.2 (Thermo Fisher Scientific) for identification and label-free precursor ion quantification. The search parameters were as follows: (a) trypsin as an enzyme with up to two missed cleavages; (b) precursor mass tolerance of 10 ppm; (c) fragment mass tolerance of 0.02 Da; and (d) acetylation of protein N-terminus, oxidation of methionine, and deamidation of asparagine and glutamine as variable modifications. Peptides were filtered at a false-discovery rate of 1% using the percolator node. Normalization was performed such that the total sum of abundance values for each sample over all peptides was the same. The MS proteomics data of BioID2 were deposited to the ProteomeXchange Consortium via the jPOST partner repository (https://repository.jpostdb.org) with the dataset identifiers JPST000527/PXD011939, JPST000529/PXD011946, and JPST000618/PXD014218 (Okuda et al., 2017).

**Cross-linking mass spectrometry**

In a 10-cm dish, mitochondria were isolated from confluent HEK293 cells stably expressing PHB2(V1) or PHB1 with a C-terminal 3×Myc tag, and resuspended in a cross-linking buffer [1× PBS (pH 7.4) and 50 or 100 μM DSBU (Thermo Fisher Scientific)] for 30 min at room temperature. After the cross-linking reaction, the resultant proteins were incubated with 50 mM Tris-HCl (pH 7.5) for 15 min at room temperature to quench the excess DSBU. The cross-linked mitochondria were then lysed in 600 μL of RIPA buffer for 1 h at 4° C, followed by centrifugation at 15,000 *g* for 10 min. The clarified supernatants were incubated with 20 μL of anti *c*-Myc agarose beads, followed by washing three times with 1× PBS (pH 7.4) and twice with 50 mM ammonium bicarbonate. Proteins on the beads were digested by adding 400 ng trypsin/Lys-C mix for 16 h at 37° C. The digests were desalted using GL-Tip SDB, and the eluates were evaporated in a SpeedVac concentrator.

The resultant peptides were divided into two halves and subjected to LC-MS/MS analysis using both Q Exactive Plus and Orbitrap Fusion Lumos mass spectrometers with the EASY-nLC 1200 systems. Raw data were analyzed using Proteome Discoverer version 2.2 with the XlinkX node (Liu et al., 2017) to identify cross-linked peptides. The MS proteomics data of cross-linking MS were deposited to the ProteomeXchange Consortium via the jPOST

partner repository with the dataset identifier JPST000528/PXD011941 and JPST000617/PXD014217.

**Confocal microscopy**

Cells were plated on coverslips in 12-well plates ($5 \times 10^4$ cells/well). The following day, the cells were fixed with 4% paraformaldehyde for 10 min, permeabilized with 0.2% Triton X-100 in 1× PBS (pH 7.4), and blocked with 5% BCS. Epitope tagged PHB2 proteins (HA- or Myc-) were detected with its specific polyclonal primary and AlexaFluor488 secondary antibodies, and mitochondria were stained with anti-mtHSP70 primary antibody followed by the Cy3-conjugated secondary antibody. In some experiments, cells were incubated with 150 nM MitoTracker Red CMXRos for 1 h before fixation and then followed the same process described above (monitoring the $\Delta\Psi_m$). Cells were imaged with a $C2^+$ confocal microscope (Nikon Instruments Inc).

**Electron microscopy**

For electron microscopy, cells were fixed in 100 mM cacodylate buffer (pH 7.4) containing 2% paraformaldehyde and 2% glutaraldehyde for 1 h, washed and fixed again with 100 mM cacodylate buffer containing 2% glutaraldehyde overnight at 4° C. After fixation, the cells were washed 4 times with 100 mM cacodylate buffer for 20 min each, and post-fixed with 2% osmium tetroxide ($OsO_4$) in cacodylate buffer at 4° C for 1 h. Cells were then dehydrated in a graded series of ethanol (50%, 70%, 90%, and 100%), embedded in resin (Quetol 812, Nisshin EM Co, Japan), and polymerized at 60° C for 48 h. The polymerized resins were cut in ultra-thin sections at 70 nm with an LEICA UTC ultramicrotome, mounted on copper grids, and stained with 2% uranyl acetate and lead solution (Sigma-Aldrich). Images were collected with a transmission electron microscope (JEM-1400Plus; JEOL Ltd, Japan) operating at 80 kV and equipped with a CCD camera (VELETA; Olympus Soft Imaging Solutions GmbH, Germany).

**RNA interference**

For RNA interference knockdown experiments, 21-nucleotide siRNAs were purchased from Thermo Fisher Scientific (Silencer Select Custom siRNA Library). HEK293 (or A549/HeLa) cells were each transfected with 10 nM siRNA (final concentration) three times within 48 h using Lipofectamine RNAiMAX (Thermo Fisher Scientific) following the manufacturer's protocols. At 72 h after the initial treatment, the siRNA-treated cells were used for some functional assays. Silencer Select Negative Control No. 1 siRNA was used as the control.

**Dual luciferase reporter assay**

HEK293 cells ($3 \times 10^5$ cells/well) pre-treated with siRNAs were plated in 24-well plates. The following day, cells were co-transfected with 100 ng of a luciferase reporter plasmid p125luc, 2.5 ng of the Renilla luciferase internal control vector phRL-TK (Promega), and each of the indicated expression plasmids using Lipofectamine 2000 reagent (Thermo Fisher Scientific) following the manufacturer's protocols. Empty vector [pcDNA3.1(-)] (Invitrogen) was used to maintain equivalent amounts of DNA in each well. Cells were harvested 24 h post-transfection, and analyzed by a dual-luciferase reporter assay on the GloMax 20/20n luminometer (Promega). Each experiment was replicated at least three times.

**ELISA**

Production of IFN-β was measured with species-specific enzyme-linked immunosorbent assay (ELISA) reagents for human and murine IFN-β from Kamakura Techno-Science Inc. and R&D Systems, respectively. Murine IL-6 was measured using its specific antibody from eBioscience.

**Immunoprecipitation**

For co-immunoprecipitation experiment, HEK293 cells at 80% confluence were transiently transfected with the appropriate plasmids (2 μg each) in a six-well plate by the calcium phosphate method. Two days after transfection, cells were lysed with 1 mL lysis buffer containing 50 mM Tris-HCl (pH 7.4), 150 mM NaCl, 10% (w/v) glycerol, 1% NP-40, and protease inhibitor cocktail and the clarified supernatants were incubated for 6 h at 4° C with 20 μL of agarose beads conjugated to a polyclonal antibody against *c*-Myc. After four washes with 1× PBS (pH 7.4), the immunoprecipitates were resolved by 8% or 10% SDS-PAGE and immunoblotted with the anti-HA monoclonal antibody HA.11.

To immunoprecipitate endogenous MAVS, HEK293 cells stably expressing Myc-tagged CLPB were infected with or without SeV (4 HA units/mL) overnight at 37° C. The following day, the cells were washed once with 1× PBS (pH 7.4), lysed with lysis buffer containing 50 mM Tris-HCl (pH 7.4), 150 mM NaCl, 10% (w/v) glycerol, 1 mM EDTA, and 0.5% (w/v) digitonin, protease inhibitor cocktail, and the clarified supernatants were incubated with 2 mg of the anti-*c*-Myc monoclonal antibody 9E10 followed by incubation overnight at 4° C with 20 μL of protein A-Sepharose beads. The beads were washed four times with 1× PBS (pH 7.4), and the immunoprecipitates were resolved by 8% SDS-PAGE and immunoblotted with the anti-MAVS polyclonal antibody.

**Cytochemical analysis of COX activity**

COX staining was performed as previously described (Yoshizumi et al. 2017) with slight modifications. In brief, cells plated on 18-mm coverslips were fixed with 2% paraformaldehyde in 1× PBS (pH 7.4) for 15 min and washed twice with 1× PBS (pH 7.4) for 5 min each. To visualize COX activity, cells were stained with 100 mM phosphate buffer (pH 7.4) containing 0.6 mg/mL 3',3'-diaminobenzidine, 0.3 mg/mL cytochrome *c*, and 45 mg/mL sucrose for 2 h at 37° C. Cells were then washed twice with 0.1 M Tris-HCl buffer (pH 8.0) for 5 min each and analyzed by microscopy.

**Quantification and Statistical Analysis**

Two-tailed Student's *t* tests were used for comparisons of two samples. All statistical analyses were performed in GraphPad QuickCalcs (GraphPad Software). Data are presented as mean ± standard error (SEM). The statistical tests used and the number of biologic replicates is indicated in each figure legend. Statistical significance was defined as a *p* value of less than 0.05. No methods were used to determine whether the data met the assumptions of the statistical approach.

## Data and Software Availability

Refined $PHB2^{188\text{-}265}$ crystal structure; Protein Data Bank (PDB ID: 6IQE)

BioID2 data [Control, PHB2(V1), PHB2(V3)]; Japan ProteOme STandard Repository/Database (jPOST) (JPST000527/PXD011939)

BioID2 data ($PHB2^{WT}$, $PHB2^{I225P}$, $PHB2^{KKK}$); jPOST (JPST000529/PXD011946)

BioID2 data (MAVS, CLPB, PHB1); jPOST (JPST000618/PXD014218)

Cross-linking MS data; jPOST (JPST000528/PXD011941 and JPST000617/PXD014217)

## Supplemental References

Adams, P.D., Afonine, P.V., Bunkóczi, G., Chen, V.B., Davis, I.W., Echols, N., Headd, J.J., Hung, L.W., Kapral, G.J., Grosse-Kunstleve, R.W., et al. (2010) PHENIX: a comprehensive Python-based system for macromolecular structure solution. Acta Cryst. D66, 213–221.

Edelhoch, H. (1967) Spectroscopic determination of tryptophan and tyrosine in proteins. Biochemistry *6*, 1948-1954.

Emsley, P., Lohkamp, B., Scott, W.G., and Cowtan, K. (2010) Features and development of Coot. Acta Crystallogr. D Biol. Crystallogr. *66*, 486-501.

Gilquin, B., Taillebourg, E., Cherradi, N., Hubstenberger, A., Gay, O., Merle, N., Assard, N., Fauvarque, M.O., Tomohiro, S., Kuge, O., and Baudier, J. (2010) The $AAA^+$ ATPase ATAD3A controls mitochondrial dynamics at the interface of the inner and outer membranes. Mol. Cell. Biol. *30*, 1984-1996.

Janke, C., Magiera, M.M., Rathfelder, N., Taxis, C., Reber, S., Maekawa, H., Moreno-Borchart, A., Doenges, G., Schwob, E., Schiebel, E., et al. (2004) A versatile toolbox for PCR-based tagging of yeast genes: new fluorescent proteins, more markers and promoter substitution cassettes. Yeast *21*, 947-962.

Kabsch, W. (2010) XDS. Acta Crystallogr. D Biol. Crystallogr. *66*, 125-132.

Liu, F., Lössl, P., Scheltema, R., Viner, R., and Heck, A.J.R. (2017) Optimized fragmentation schemes and data analysis strategies for proteome-wide cross-link identification. Nat. Commun. *8*, 15473.

Lorenz, M.C., Muir, R.S., Lim, E., McElver, J., Weber, S.C., and Heitman, J. (1995) Gene disruption with PCR products in *Saccharomyces cerevisiae*. Gene *158*, 113-117.

Miyata, N., Goda, N., Matsuo, K., Hoketsu, T., and Kuge, O. (2017) Cooperative function of Fmp30, Mdm31, and Mdm32 in Ups1-independent cardiolipin accumulation in the yeast *Saccharomyces cerevisiae*. Sci. Rep. *7*, 16447.

Okuda, S., Watanabe, Y., Moriya, Y., Kawano, S., Yamamoto, T., Matsumoto, M., Takami, T., Kobayashi, D., Araki, N., Yoshizawa, A.C., et al. (2017) jPOSTrepo: an international standard data repository for proteomes. Nucleic Acids Res. *45*, D1107-D1111.

Tong, A.H., and Boone, C. (2006) Synthetic genetic array analysis in *Saccharomyces cerevisiae*. Methods Mol. Biol. *313*, 171-192.

Winn, M.D., Ballard, C.C., Cowtan, K.D., Dodson, E.J., Emsley, P., Evans, P.R., Keegan, R.M., Krissinel, E.B., Leslie, A.G., McCoy, A., et al. (2011) Overview of the CCP4 suite and current

developments. Acta Crystallogr. D Biol. Crystallogr. *67*, 235-242.

Yoshizumi, T., Ichinohe, T., Sasaki, O., Otera, H., Kawabata, S., Mihara, K., and Koshiba, T. (2014) Influenza A virus protein PB1-F2 translocates into mitochondria via Tom40 channels and impairs innate immunity. Nat. Commun. *5*, 4713.

Zhu, J., Vinothkumar, K.R., and Hirst, J. (2016) Structure of mammalian respiratory complex I. Nature *536*, 354-358.